

# SPATIAL GENERATION OF ELECTRON EXCITATIONS ON THE X-RAY ABSORPTION

V.YA. DEGODA, A.O. SOFIENKO

UDC 535.37  
©2007

Taras Shevchenko Kyiv National University  
(2, build. 1, Academician Glushkov Ave., Kyiv 03608, Ukraine; e-mail: degoda@univ.kiev.ua)

We present a model of the spatial distribution of electron excitations which are generated during the deceleration of a high-energy photoelectron created under the X-ray quantum absorption in a medium. It is shown that the resultant distribution can be presented in a form of the analytic dependence on the medium parameters and the photoelectron energy. The obtained result has the large importance for the kinetics of X-ray conduction and X-ray luminescence, where the essential point is the consideration of the spatial inhomogeneity of excitations, and for the calculation of the spatial distribution of the X-ray fluorescence in a material during the irradiation by high-energy electrons.

distribution of generated excitations caused by the high-energy (in comparison with the work function or the forbidden bandwidth value) photoelectron thermalization. The photoelectron thermalization time period constitutes  $\sim 10^{-13}$  s [5] that is much less than the duration of scintillation and recombination processes. Approximately one third of the energy of a photoelectron is consumed in the generation of electron excitations [5, 6] because of the inelastic scattering by ions, and its major part is consumed to generate the oscillations of ions (phonons) by the elastic scattering.

## 1. Introduction

The considerably inhomogeneous spatial generation of electron excitations determines the specific differences between XL and photoluminescence. During the registration of an X-ray quantum with an energy of 1–50 keV, the dominating process of its interaction with the substance is the photoabsorption. As a result of the absorption, the quantum energy (with regard for the loss due to internal *K*- or *L*-shell ionization) is transferred to a recoil electron, i.e. a photoelectron. At the thermalization of the photoelectron, a part of the kinetic energy is consumed to generate electron excitations (free charge carriers, excitons), and the remaining energy portion is transformed to heat directly. In this case, the radial displacement of a photoelectron is smaller by tens of times than its entire traveled path (the straightened path length) due to the scattering by ions of the substance. This is the cause of a certain localization of excitations generated by a photoelectron in space, which influences, of course, their further relaxation (recombination) kinetics.

In the existing kinetic theory of XL [1–4], it is assumed that, in the local area where the electron excitations are generated in case of the absorption of an X-ray quantum with an energy of 1–50 keV, the total number of traps and recombination centers is much less than the number of generated excitations. This fact allows using the  $\delta$ -function as the initial

The behavior of electrons after several collisions can be considered on the base of the multiple scattering theory. At the great number of collisions, their motion directions are distributed, in fact, according to the random law, when the diffusion standard equations can be used [7, 8]. An increase in the frequency of inelastic collisions with heavy elements (large *Z*) is the reason for that the diffusion character of the motion of electrons is installed significantly faster than in the case of light elements. Experimental studies of the inverse scattering of electrons in substances with various *Z* also showed the significant influence of the single scattering of electrons on their motion trajectory. In work [9], it was even proposed the empiric formula for the coefficient of inverse scattering of electrons with energies of 10–30 keV which achieves, e.g., 18 % for silicone. The numerical methods of simulation of the trajectories of high-energy electrons by the Monte-Carlo method [10–12] confirmed it as well.

Thus, if the diffusion character of the motion of a photoelectron under thermalization is established and the parameters of this motion are determined by using the Bethe–Bloch equation for ionization losses, it is possible to determine the average-statistical spatial distribution of the generated electron excitations in a crystalline phosphor, this distribution being initial for XL.

## 2. Trajectory of a High-Energy Electron under Thermalization

The high-energy photoelectron trajectory is determined by its Coulomb interaction with the valence electrons, electrons of internal filled shells, and nuclei of ions of the matrix. The quadratic dependence of the Coulomb field on the distance allows one to consider that the interactions of an electron with ions close to its trajectory are the actions independent of one another. This assumption is confirmed by the fulfilment of the following condition: the de Broglie wavelength of high-energy electrons is by many times less than the average distance between ions. Certainly, the laws of momentum and energy conservation should be fulfilled during the elastic and/or inelastic interaction at each act of the scattering of an electron by an ion. Also it is necessary to remember that, during the electron-ion scattering, there occurs the bremsstrahlung radiation of electromagnetic waves due to the deceleration of the electron (by the bremsstrahlung radiation generation mechanism in an X-ray tube) which can be absorbed by valence electrons. Definitely, the bremsstrahlung radiation absorption determines the inelastic scattering mechanism. The numerical analysis of the elastic scattering of the electron by ions of the matrix with the use of the Coulomb interaction model shows that only if the electron energy is tens of keV and the impact parameter is extremely small, the electron can transfer an energy of several eV to an ion, i.e. the energy sufficient for the generation of a single electron excitation. Therefore, this mechanism of losses of the electron kinetic energy under thermalization can be hardly dominating, which is determined, in the first turn, by the ratio of the electron mass to the ion mass.

On the interaction of a high-energy electron with the electrons of internal filled shells, it cannot transfer the additional small energy and momentum to these electrons as they are located on the discrete energy levels of an ion. In fact in this case the additional energy and momentum is consumed by the massive ion, and the elastic scattering remains dominating. Although the probability of the inelastic scattering is small but it doesn't equal zero, which is confirmed by the observation of the characteristic radiation of X-ray tubes.

The minimum energy which can be obtained by the valence electron on the interaction with a photoelectron is equal to  $E_g$  (forbidden bandwidth). But if the elastic scattering takes place, the recoil energy and momentum is again obtained by the ion, and this additional energy causes an increase in the amplitude of ion's oscillations,

i.e. this energy is transformed directly to heat. Thus, at the elastic scattering when the energy loss of a high-energy electron is smaller than  $E_g$ , the scattering occurs on the ion, and the scattering angle will be small. On the contrary, at the inelastic scattering of a high-energy electron, two free particles (electron and hole) are generated, and the scattering angle of a photoelectron will be virtually the same in all directions. This statement rather satisfactorily correlates with characteristics of the radiation in X-ray tubes, where the total intensity of the radiation is directly proportional to the number of a chemical element  $Z$ . Since the elastic scattering will occur in the most cases, the motion trajectory of a high-energy electron at thermalization will have the form of rectilinear segments between the inelastic scattering events and arbitrary changes of directions between them.

Also we note that the total number of electron excitations  $N_0$ , which are generated at a single X-ray quantum absorption ( $h\nu_X$ ), is expressed by the phenomenological dependence [5,6]

$$N_0 = \frac{h\nu_x}{(2.5 \div 3)E_g}. \quad (1)$$

It allows determining the total energy lost by the photoelectron at elastic scatterings and a single inelastic scattering  $W_0$  on the lattice ions:

$$W_0 \approx 3E_g, \quad (2)$$

i.e. the energy lost on one segment of its trajectory.

Such special features of the interaction of a high-energy electron with the substance ions testify that the electron motion trajectory at thermalization can be compared with the trajectories of atoms in gases, i.e. with the diffusion in gases. The important confirmation of the diffusion motion is the scattering uniformity in any direction at the interaction. In this case (for example, the diffusion of atoms in gases), there are no restrictions on the energy of diffusing particles. Therefore, using the model of photoelectron diffusion displacement at thermalization is rightful.

## 3. High-Energy Electron Diffusive Motion Parameters

The diffusive character of the motion of a high-energy electron in the process of its thermalization allows using the diffusion equation to calculate the average-statistical probability of the location of the electron in space at each time instant and definitely at the time instants of

non-elastic interactions when the electronic excitations are generated. Thus, if we determine the probability of the location of a high-energy electron in space at time instants of the inelastic scattering, it is possible to obtain the average-statistical spatial distribution during the thermalization of a photoelectron by integrating over the time.

As the kinetic energy of a high-energy electron gradually decreases, the diffusion coefficient  $D$  will change during the thermalization as well. In general case, it is determined as

$$D = 1/3L(t)v(t), \quad (3)$$

where  $L(t)$  is the free path length (the spatial distance between two events of the electron excitation generation), and  $v(t)$  is the photoelectron velocity which gradually decreases during the thermalization. The introduction of the dependence of the diffusion coefficient on the free path length is based on the fact that the kinetic parameters of a motion don't change practically on elastic collisions. This assumption only increases the diffusion coefficient and consequently increases the space volume, where the photoelectron is thermalized and the electronic excitations are generated. The introduction of the dependence of the diffusion coefficient on the path length, where it creates a single electron-hole pair, is based on the fact that, in this case, the kinetic parameters of the motion of the electron change, as distinct from the case of elastic collisions, when only the propagation direction is changed.

Let's consider how the quantities  $L(t)$  and  $v(t)$  depend on time. The photoelectron velocity is determined by its kinetic energy, by assuming that the electron is non-relativistic:

$$v(t) = \sqrt{\frac{2}{m}E(t)} = \sqrt{\frac{2}{m}E[x(t)]}. \quad (4)$$

The dependence of the electron energy on the passed distance  $x(t)$  is described by the Bethe–Bloch equation [8] for the non-relativistic electron ionization losses. This equation in SI looks as follows:

$$-\frac{dE}{dx} = \frac{e^4 n}{8\pi\epsilon_0^2 E} \ln\left(\frac{4E}{\bar{I}}\right),$$

where  $n$  is the concentration of electrons in the substance ( $n = \frac{Z\rho N_A}{A}$ ,  $Z$  is the atomic number and  $A$  is the atomic mass,  $\rho$  is the density,  $N_A$  is the Avogadro number);  $\bar{I}$  is the average ionization potential of the substance which approximately equals  $4E_g$  for the majority of classical crystalline phosphors and semiconductors. So

the expression under the logarithm symbol will be proportional to the number of events of the ionization or the generation of electronic excitations which are created by a high-energy electron with energy  $E$ . In our case, this quantity will be equal to  $3(N_0 - N)$  according to (1) and (2). Substituting the numerical values of the electron charge  $e$  and the dielectric permittivity  $\epsilon_0$  and using the units (nm, eV) more suitable for calculations, we have

$$\frac{dE}{dx} \left( \frac{\text{eV}}{\text{nm}} \right) = 13 \frac{n(\text{cm}^{-3}) \times 10^{-24}}{E(\text{keV})} \ln[3(N_0 - N)]. \quad (5)$$

In the general case, the integration of (5) doesn't give a simple analytic expression. But, to obtain the approximate dependence of the photoelectron energy upon the straightened path length ( $x$ ), it is possible to use the fact that the logarithmic dependence of  $E$  changes much slower than the power function of  $E$ . Hence, using the theorem of mean from the calculus, we have

$$\int_0^x dx = x = - \frac{\int_{E_0}^{E(x)} E dE}{13 \cdot 10^{-24} n \ln 3 (N_0 - N)} \approx \approx \frac{E_0^2 - E^2(x)}{2A}, \quad A = \frac{e^4 n \ln N_0}{8\pi\epsilon_0^2}, \quad (6)$$

$$\begin{aligned} \overline{\ln 3(N_0 - N)} &= \frac{N_0 \ln 3 + \ln N_0!}{N_0} \approx \\ &\approx \frac{N_0 \ln 3 + N_0 (\ln N_0 - 1)}{N_0} \approx \ln N_0. \end{aligned}$$

The constant  $A$  can change only by several times while changing  $E$  by orders. The obtained expression allows determining the total straightened path length of a high-energy electron on the thermalization as

$$x_0 = \frac{E_0^2 - W_0^2}{2A} \approx \frac{E_0^2}{2A}, \quad (7)$$

that is the same as the known Thompson-Waddington relation [13]. Using (7), it is possible to write the approximate analytic dependence of the photoelectron energy on the passed distance:

$$E(x) = E_0 \sqrt{1 - x/x_0}. \quad (8)$$

Using this expression and (4), we get the equation for  $x(t)$  and  $v(t)$  :

$$v(x) = (2E_0/m)^{1/2} (1 - x/x_0)^{1/4} = v_0 (1 - x/x_0)^{1/4},$$

$$v(t) = v_0 (1 - t/t_0)^{1/3} \left( v_0 = \sqrt{2E_0/m} \right); \quad (9)$$

$$t(x) = \int_0^x \frac{dx}{v(x)} = \frac{4x_0}{3v_0} \left[ 1 - (1 - x/x_0)^{3/4} \right],$$

$$x(t) = x_0 \left[ 1 - (1 - t/t_0)^{4/3} \right]. \quad (10)$$

The photoelectron thermalization total time ( $t_0$ ) is determined from the condition  $x \rightarrow x_0 : t_0 = \frac{4x_0}{3v_0}$ . The dependence  $L(x)$  or  $L(t)$  is obtained from the condition that, at this distance, a photoelectron creates a single electronic excitation, i.e. it loses the energy  $W_0 \approx 3E_g$  :

$$L(x) = \frac{2W_0 x_0}{E_0} \sqrt{1 - x/x_0},$$

$$L(t) = \frac{2W_0 x_0}{E_0} (1 - t/t_0)^{2/3},$$

$$L_0 = 2W_0 x_0/E_0 = 2x_0/N_0. \quad (11)$$

Thus, for the diffusion coefficient of the photoelectron, we have the analytic formula

$$D(x) = D_0 (1 - x/x_0)^{3/4}, \quad D(t) = D_0 (1 - t/t_0), \quad (12)$$

where

$$D_0 = \frac{\sqrt{2} W_0 E_0^{3/2}}{3 A m^{3/2}}.$$

The obtained parameters of the diffusion motion of a high-energy electron during the thermalization process allow determining the spatial kinetics of generation of the electronic excitations.

#### 4. Kinetics of Generation of Electronic Excitations

To describe the diffusion motion of various particles in a substance, the notion of their concentration  $N(r, t)$

is used. The equation describing their diffusion is the following:

$$\frac{dN(r, t)}{dt} = \nabla[D \nabla N(r, t)]. \quad (13)$$

It is obtained while considering the probability of the transition of particles through a unit cross section per unit time. Solving the diffusion equation gives the values of the concentration of particles in space at a certain time instant. The necessary condition for a solution of the diffusion equation (13) to be obtained is the initial condition: the spatial distribution of the concentration at the initial time instant  $t=0$ :  $N(r, 0) = N_0 \varphi(r)$  . The diffusion equation is used, as a rule, for the great number of similar particles that allows obtaining the average-statistical kinetics of a spatial distribution of their concentration. But the diffusion equation itself determines only the probability of the presence of diffusing particles in a volume element at the given time instant. The solution of the diffusion equation for a single particle determines the probability of its location at the given place at each time instant. The expression  $N(r, t)/N_0 = p(r, t)$  is the probability density which specifies the corresponding concentration distribution in space at a certain time instant. While integrating  $p(r, t)$  over the entire spatial co-ordinates at any time instant, we should get unity. Actually,  $p(r, t)$  doesn't depend on the concentration of particles and determines their spatial distribution only. It is easy to obtain the diffusion equation for the spatial distribution probability density if we divide both the sides of (13) by  $N_0$  :

$$\frac{dp(r, t)}{dt} = \nabla[D(t) \nabla p(r, t)]. \quad (14)$$

To thermalize the photoelectrons, it is necessary to take into account the dependence of the diffusion coefficient on the thermalization time. Its parametrization by the passed distance rather than by time will be incorrect, because, at the diffusion displacement, the electron velocity  $v(t)$  and the path value  $L(t)$  (with respect to non-elastic interactions) are of the essential significance, rather than the place where the electron is located in space. Furthermore, each trajectory is individual, and the location in space is the statistical process, whereas only the average-statistical quantities are considered in the diffusion equation. During the thermalization of the photoelectrons with the same energy, there is no difference if one considers the simultaneous motion of some number of photoelectrons or the individual motion of each electron, because their motion is always independent. Therefore, the main

information on their location in space at a certain time instant from the beginning of the motion will be provided by just the probability density  $p(r, t)$ . Therefore, by assuming that their some number at the initial time instant is described by the spatial distribution in the form of the  $\delta$ -function, we get the solution of the diffusion equation that will be also true in the case of the motion of a single particle. The experimental registration of X-ray photons and the thermalization of photoelectrons have the individual character in each individual interaction event. But, because there occurs the significant number of events per unit time, we will consider the statistical averaging over the registration results for the totality of particles as the result of the thermalization of a single particle.

Taking into account the material homogeneity and the symmetry relatively to a direction, we will determine the radial displacement only. In this case, we have the diffusion equation and the initial condition:

$$\begin{cases} \frac{dp(r, t)}{dt} = D_0 \left(1 - \frac{t}{t_0}\right) \Delta p(r, t) \\ p(r, 0) = \delta(r), \end{cases} \quad (15)$$

where  $r$  is a distance from the initial point of the motion, i.e. from the place of the X-ray quantum absorption. Equation (15) can be solved by separating the variables  $r$  and  $t$  [14], which splits the diffusion equation into two individual equations: one for the time variables and the second for the spatial variables. The general solution of the diffusion equation looks, after some easy calculations, as follows:

$$p(r, t) = \frac{\exp\left\{-\frac{r^2}{2D_0t_0[1-(1-t/t_0)^2]}\right\}}{\left\{2\pi D_0t_0\left[1-\left(1-\frac{t}{t_0}\right)^2\right]\right\}^{3/2}}. \quad (16)$$

Thus, we get the analytic equation to determine the probability of the location of a high-energy electron in space as a function of time during the thermalization process.

## 5. Calculation of the Spatial Distribution of Electronic Excitations

The calculation of the spatial distribution of electronic excitations can be carried out by using the obtained relation (16). The probability of the event that, at a certain time instant ( $t_i$ ), the electron-hole pair will be generated is proportional to the probability of the location of a photoelectron there. The complete distribution of pairs generated by a photoelectron can

be found as the additive sum over  $i$  from 1 to  $N_0$  of the probability densities:

$$N_0(r) = \sum_{i=1}^{N_{\max}} p(r, t_i). \quad (17)$$

We note that though the electronic excitations are generated by a high-energy electron discretely in space, the condition  $N_0 \gg 1$  is satisfied for all luminophores on the X-ray excitation, which yields the practically identical spatial distributions of electronic excitations. This is confirmed by the calculation results of the deceleration of high-energy electrons used in the electron-probe microanalysis in metals, by using the Monte-Carlo method [15]. Therefore, using the probability density of the generation of electron-hole pairs provides their average-statistical spatial distribution in a material. The instants of electronic excitations ( $t_i$ ) can be found from the condition that, in each time interval from  $t_i$  to  $t_{i+1}$ , the photoelectron loses the energy  $W_0$ :

$$E(t_i) = E_0 - iW_0.$$

Using expressions (8) and (10), we get

$$t_i = t_0 \left[1 - (1 - iW_0/E_0)^{3/2}\right]. \quad (18)$$

Thus, the spatial distribution of electronic excitations  $N_0(r)$  has the form

$$N_0(r) = \sum_{i=1}^{N_0} \frac{\exp\left\{-\frac{r^2}{2D_0t_0[1-(1-iW_0/E_0)^3]}\right\}}{\left\{2\pi D_0t_0\left[1-\left(1-iW_0/E_0\right)^3\right]\right\}^{3/2}}. \quad (19)$$

Because this formula includes the sum of  $N_0$  terms, it is possible to return to the Bethe–Bloch equation and try to obtain a more accurate result for relations (6)–(8), but not in the analytic form. If we divide the integral in (6) into a sum of  $N_0$  integrals over  $E(x)$  because we have the uniform step  $\Delta E = W_0$ , then the conducted analysis testifies that the  $E(x)$  determination accuracy is beyond the 2abandon the obtained analytic relations for  $E(x)$  and  $x(t)$  and, respectively, for  $v(t)$  and  $D(t)$ .

Hence, for the generation stage of the kinetic theory of X-ray luminescence and X-ray conduction, we have the calculation system of the initial spatial distribution of the density  $N_0(r)$  of electron excitations which are generated in a substance at the absorption of a single X-ray quantum.

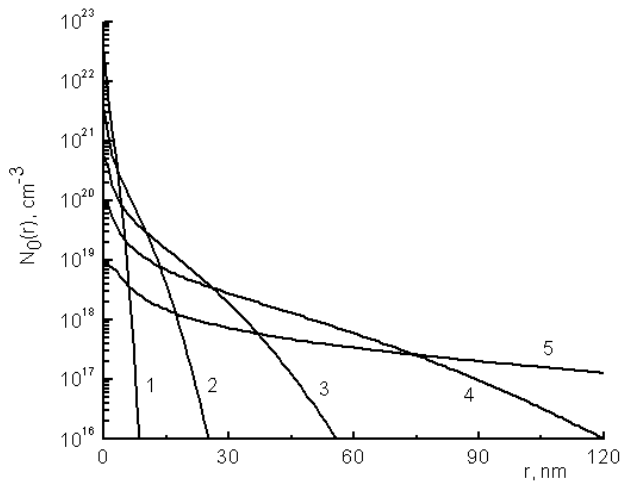


Fig. 1. Spatial distributions of the concentration  $N_0(r)$  of excitations in the material ( $n = 1.0 \times 10^{24} \text{ cm}^{-3}$  and  $E_g = 3.0 \text{ eV}$ ) for different initial energies  $E_0$ : 2 (1), 5 (2), 10 (3), 20 (4), and 50 keV (5)

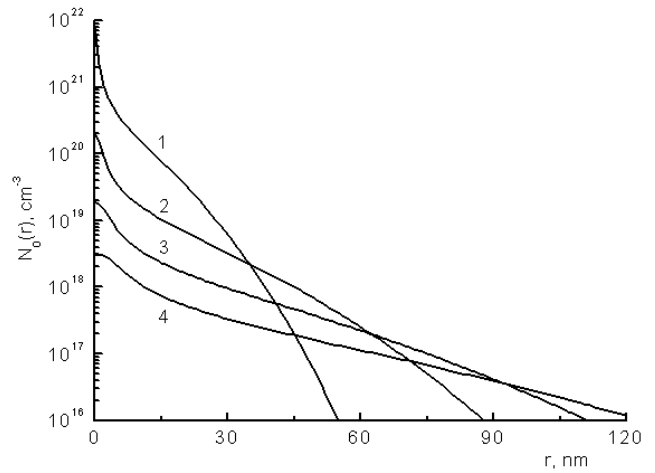


Fig. 3. Spatial distributions of the concentration of excitations  $N_0(r)$  for the initial energy  $E_0 = 15 \text{ keV}$  in materials with different forbidden bandwidths  $E_g$ , eV: 1.0 (1), 3.0 (2), 6.0 (3), and 10.0 (4) ( $n = 1.0 \times 10^{24} \text{ cm}^{-3}$ )

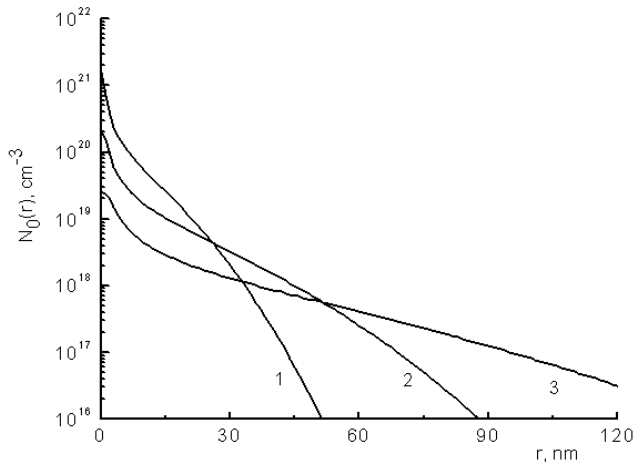


Fig. 2. Spatial distributions of the concentration of excitations  $N_0(r)$  for the initial energy  $E_0 = 15 \text{ keV}$  in materials with different electron concentrations  $n$ ,  $\times 10^{24} \text{ cm}^{-3}$ : 0.5 (1), 1.0 (2), and 2.0 (3) ( $E_g = 3.0 \text{ eV}$ )

### 6. Influence of the Ionization Losses Parameters in a Substance on $N_0(r)$

The ionization losses of the energy of photoelectrons are determined, according to the Bethe–Bloch formula, by the initial energy of a high-energy electron  $E_0$ , the electron concentration in a substance  $n$ , and the forbidden bandwidth  $E_g$ . These ionization losses of

energy, in their turn, determine the spatial distribution of generated electronic excitations. The calculated spatial distribution of the concentration  $N_0(r)$  of excitations for different initial energies of a photoelectron are shown in Fig. 1. It is clear that the maximum concentration of electron excitations will be at the center, and it increases when the initial energy  $E_0$  decreases. This is caused by the fact that the photoelectron energy loss is inversely proportional to the electron energy itself. Note that the concentrations of electron excitations considerably exceed, by the order of magnitude, the concentrations of non-controlled defects in crystals. Furthermore, these concentrations even exceed the concentrations of excitations at the irradiation by picosecond lasers. The significant influence on the space distribution  $N_0(r)$  is rendered by the concentration of electrons in a substance (Fig. 2). The increase in the concentration of electrons by several times causes the increase by orders in the maximum concentration of electronic excitations and significantly reduces the generation volume. The influence of the forbidden bandwidth  $E_g$  on  $N_0(r)$  is specified by two factors: the total number of excitations  $N_0$  and the increase of the average-statistical path length of a photoelectron between two ionization events (Fig. 3). To evaluate the volume where the electronic excitations are generated, the spatial distribution can be characterized by the dependence of the relative number of excitations which

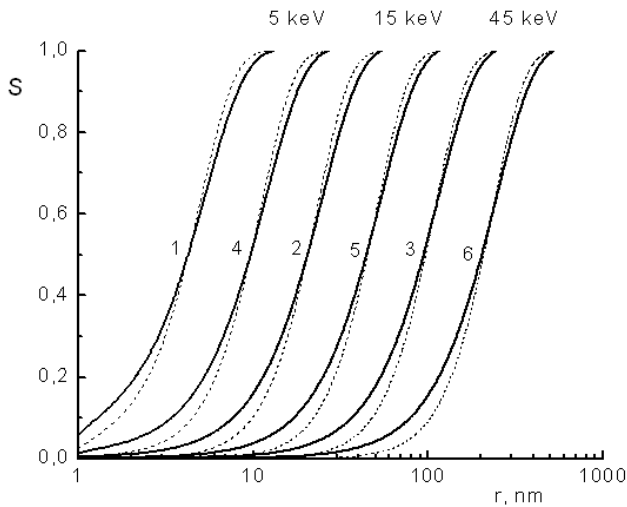


Fig. 4. Dependences  $S(r)$  for spatial distributions (19) (continuous curves) and (21) (dotted curves) for the initial energy  $E_0$ , keV: 5 (1, 4), 15 (2, 5), and 45 (3, 6) in materials with  $n = 1.5 \times 10^{24} \text{ cm}^{-3}$  (1, 2, 3) and  $n = 0.7 \times 10^{24} \text{ cm}^{-3}$  (4, 5, 6), at  $E_g = 3.0 \text{ eV}$

are generated in a sphere of radius  $r$ :

$$S(r) = \frac{\int_0^r N_0(r) 4\pi r^2 dr}{N_0}. \quad (20)$$

These calculated dependences are shown in Fig. 4. Generally, the region where electronic excitations appear at the single X-ray quantum absorption can be evaluated by the volume where 90 % of the generated excitations occur ( $S(r_{0.9}) = 0.9$ ). Such dependences shown in Fig. 5 confirm that the excitation region increases with the initial energy of a photoelectron. In this case, the larger the forbidden bandwidth of materials, the larger the excitation region. But in all cases, this region remains considerably smaller than the relaxation region of electronic excitations.

The resultant spatial distribution of the generated excitations is rather satisfactorily approximated by the function

$$N_0(r) = \frac{N_0}{(2\pi)^{3/2} r_g^3} \exp\left(-\frac{r^2}{2r_g^2}\right) \quad (21)$$

which is characterized by only one parameter. This parameter  $r_g$  is determined by the relationship

$$r_g = \frac{6\pi \varepsilon_0^2 \sqrt{E_g E_0^3}}{e^4 n \ln(E_0/(3E_g))} \Rightarrow r_g (\text{nm}) = 1.5 \frac{\sqrt{E_g (\text{eV}) E_0^3 (\text{keV})}}{[n (\text{cm}^{-3}) \times 10^{-24}] \ln(E_0/(3E_g))}. \quad (22)$$

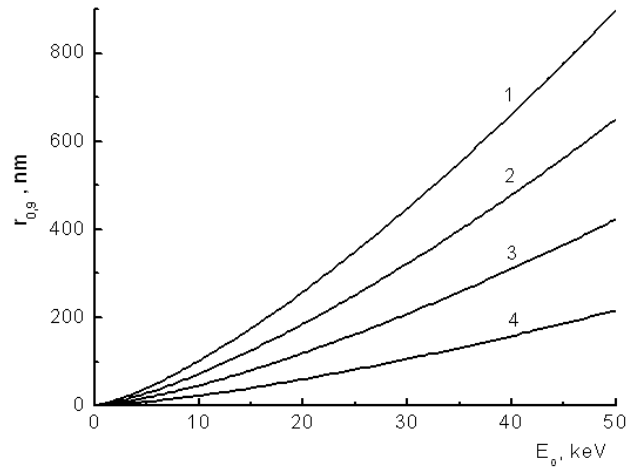


Fig. 5. Radius  $r_{0.9}$  of the generation region of electronic excitations versus the X-ray quantum energy at different values of the forbidden bandwidth  $E_g$ , eV: 1.0 (1), 3.0 (2), 6.0 (3), and 10.0 (4) in materials with  $n = 1.0 \times 10^{24} \text{ cm}^{-3}$

Such Gaussians are presented in Fig. 4 (dotted curves). The deviation of Gaussians (21) from the calculated function  $N_0(r)$  is expected only in the small central region of generation and in the case of large values  $r$ , where a small part of the electronic excitations occurs. Note that the calculated spatial distributions  $N_0(r)$  are approximated better by the dependence with the exponent of  $r$  in (21) to be slightly smaller than 2. But if we take into account the further diffusion heat motion of the generated electrons and holes which is described by a Gaussian for the spatial distribution of charge carriers, there is no reason to use a more complicated function for their average-statistical initial distribution.

The results of calculations of the parameters, which determine the thermalization region of a high-energy electron for some real materials and different initial energies of electrons, are presented in the Table.

To disadvantages of the X-ray generation model, we should refer the consideration of only monoenergy photoelectrons in the calculation of the spatial distribution of electronic excitations. In fact, due to the photoelectric effect, there occurs the characteristic additional radiation from various ion shells in addition to the generation of photoelectrons with respective energies. This radiation is effectively absorbed in the environment. This causes the asymmetry of the final spatial distribution of generated electron-hole pairs. Their account significantly complicates the total

**Thermalization parameters of a high-energy electron for various real materials**

Material	$E_\gamma$ , keV	$x_0$ , nm	$t_0$ , ps	$(\frac{dE}{dx})_0$ , eV/nm	$N_0$	$r_g$ , nm
$^{14}\text{Si}$ $n_e = 0.7 \times 10^{24} \text{ cm}^{-3}$ $E_g = 1.1 \text{ eV}$	5	161	0.005	15.5	1667	3.3
	15	1286	0.025	5.8	5000	14.8
	30	4797	0.065	3.1	10000	38.6
	50	12696	0.134	2.0	16667	78.8
ZnSe $n_e = 1.43 \times 10^{24} \text{ cm}^{-3}$ $E_g = 2.8 \text{ eV}$	5	100	0.003	25.1	625	3.4
	15	783	0.015	9.6	1875	14.9
	30	2899	0.039	5.2	3750	38.6
	50	7635	0.08	3.3	6250	78.3
Diamond $n_e = 1.06 \times 10^{24} \text{ cm}^{-3}$ $E_g = 5.4 \text{ eV}$	5	138	0.005	18.0	312	6.7
	15	1068	0.021	7.0	938	29.1
	30	3930	0.053	3.8	1875	74.9
	50	10307	0.109	2.4	3125	151

calculation algorithm. But it is necessary to note that the photoelectric effect probability on all shells, except for the  $K$ -shell, doesn't exceed  $1/5$ , which determines the final error of calculations, while using the diffusion model. It is also necessary to remember that the presented model allows one to calculate the average-statistical spatial distribution  $N_0(r)$ , and each generation region will differ from the average distribution because of the chaotic motion of a photoelectron. The preliminary estimations show that the fluctuations from the average value don't exceed 10%.

## 7. Conclusions

The evaluation of the probability of the location of a photoelectron in space, if we apply the formal approach of diffusion theory, allows one to significantly simplify the calculations of the initial distribution of electronic excitations and to specify the dimensions of the region of their generation. The dimensions of the generation region of electronic excitations at the thermalization of X-ray photoelectrons are considerably less (approximately by 30 times) than the straightened path length which is calculated by the Bethe–Bloch formula. The same estimate was given in the papers concerning the statistical simulation of low-energy electrons in a medium, which confirms the relevancy of the proposed model of their diffusion movement on the deceleration. But the main point here is that the generation region of electronic excitations in the X-ray luminescence is much less than the spatial region of the relaxation of these excitations during the scintillation and phosphorescent stages.

Note that the spatial density and the generation time of electronic excitations on the single act of X-ray quantum absorption are beyond the abilities of

picosecond lasers. If we take into account that it is easy to realize the absorption up to  $10^{10}$  quanta per second in the samples at the X-ray excitation, it becomes clear that the X-ray excitation abilities in the studies greatly exceed the abilities of picosecond lasers at the luminescence excitation.

1. V.Ya. Degoda, Ukr. Fiz. Zh. **44**, 482 (1999).
2. V.Ya. Degoda, Ukr. Fiz. Zh. **45**, 1381 (2000).
3. V.Ya. Degoda, Ukr. Fiz. Zh. **45**, 1469 (2000).
4. V.Ya. Degoda, Ukr. Fiz. Zh. **46**, 105 (2001).
5. E.D. Aluker, D.Yu. Lusic, S.A. Chernov *Electronic Excitations and Radioluminescence of Alkali-Halide Crystals* (Zinatne, Riga, 1979) (in Russian).
6. A.M. Gurvich, *X-Ray Luminophors and X-Ray Screens* (Atomizdat, Moscow, 1976) (in Russian).
7. A.N. Vasil'ev, V.V. Mikhailin, *Introduction in Solid-State Spectroscopy* (Moscow State Univ., Moscow, 1987) (in Russian).
8. A.I. Abramov, Yu.A. Kazinsky, *Foundations of Experimental Methods of Nuclear Physics* (Atomizdat, Moscow, 1985), p. 85–87, 155–200 (in Russian).
9. H.E. Bishop, Proc. Phys. Soc. **85**, 855 (1965).
10. R. Shimizu, T. Ikuta, K.J. Murata, Appl. Phys. **43**, 4233 (1972).
11. T. Matsukava, K. Murata, R. Shimizu, Phys. status solidi (b) **55**, 371 (1973).
12. M. Green, Proc. Phys. Soc. **82**, 204 (1963).
13. *Physical Foundations of X-Ray Spectrum Local Analysis*, I.B. Borovsky (Ed.) (Nauka, Moscow, 1973) (in Russian).
14. N.S. Koshlyakov, E.B. Gliner, M.M. Smirnov, *Partial Differential Equations of Mathematical Physics* (Vysshaya Shkola, Moscow, 1970), p. 451–487 (in Russian).
15. S.J.B. Reed, *Electron Microprobe Analysis* (Cambridge Univ. Press, Cambridge, 1975).
16. *Tables of Physical Quantities*, I.K. Kikoin (Ed.) (Atomizdat, Moscow, 1976) (in Russian).

Received 07.07.06



ПРОСТОРОВА ГЕНЕРАЦІЯ ЕЛЕКТРОННИХ  
ЗБУДЖЕНЬ ПРИ ПОГЛИНАННІ  
РЕНТГЕНІВСЬКОГО КВАНТА

*В.Я. Дегода, А.О. Софієнко*

Р е з ю м е

Запропоновано модель розрахунку просторового розподілу електронних збуджень, які генеруються під час гальмування

високоенергетичного фотоелектрона, що виникає як наслідок поглинання рентгенівського кванта в середовищі. Показано, що кінцевий розподіл електронних збуджень можна представити у вигляді аналітичної функції від параметрів середовища та енергії фотоелектрона. Отриманий результат є важливим як для дослідження кінетики рентгенолюмінесценції та рентгенопровідності, де важливим моментом є врахування просторової неоднорідності збуджень, так і для розрахунку просторового розподілу генерації рентгенівської флуоресценції у матеріалі при опроміненні високоенергетичними електронами.